

An upstream multi-wavelength shared PON based on tunable self-seeding Fabry-Pérot laser diode for upstream capacity upgrade and wavelength multiplexing

Min Zhu,^{1,2,*} Shilin Xiao,¹ Zhao Zhou,¹ Wei Guo,¹ Lilin Yi,¹ Meihua Bi,¹ Weisheng Hu,¹ and Benoit Geller²

¹State Key Lab of Advanced Optical Communication Systems and Networks, Department of Electronic Engineering, Shanghai Jiao Tong University, 800 Dongchuan Road, Shanghai 200240, China

²UEI Lab, ENSTA Paris-Tech, 32 Boulevard Victor, 75739, Paris, France

*zhuminxuan@sjtu.edu.cn

Abstract: We proposed an Upstream Multi-Wavelength Shared (UMWS) PON architecture based on a tunable self-seeding Fabry-Perot laser diode (FP-LD) at ONU. The performances of the wavelength and power stability, side-mode suppression ratio (SMSR), tuning range for the proposed tunable self-seeding laser module at ONU are experimentally investigated. The BER is measured with direct modulation on FP-LD of 1.25 Gbps upstream data. The extensive simulations not only evaluate the enhanced performance from the upstream wavelength-sharing, but also for the first time investigate the impact of channel Switch Latency (SL) on the network performance.

©2011 Optical Society of America

OCIS codes: (140.3510) Lasers, fiber; (140.3520) Lasers, injection-locked; (060.4510) Optical communications.

References and links

1. G. Kramer and G. Pesavento, "Ethernet passive optical network (EPON): building a next-generation optical access network," *IEEE Commun. Mag.* **40**(2), 66–73 (2002).
2. K. Ohara, A. Tagami, H. Tanaka, M. Suzuki, T. Miyaoka, T. Kodate, "Traffic analysis of Ethernet-PON in FTTH trial service," OFC/NFOEC 2003 (Optical Society of America, 2003), paper ThAA2.
3. B. McDonald, "EPON deployment challenges – now and the future," OFC/NFOEC 2007 (Optical Society of America, 2007), paper JWA96.
4. Y.-L. Hsueh, W.-T. Shaw, L. G. Kazovsky, A. Agata, and S. Yamamoto, "Success PON demonstrator: Experimental exploration of next generation optical access networks," *IEEE Commun. Mag.* **43**(8), S26–S33 (2005).
5. T. Jayasinghe, C. J. Chae, and R. S. Tucker, "Scalability of RSOA-based multi-wavelength Ethernet PON architecture with dual feeder fiber," *J. Opt. Netw.* **6**(8), 1025–1040 (2007).
6. M. Attygalle, Y. J. Wen, J. Shankar, A. Nirmalathas, X. Cheng, and Y. Wang, "Increasing upstream capacity in TDM-PON with multiple-wavelength transmission using Fabry-Perot laser diodes," *Opt. Express* **15**(16), 10247–10252 (2007).
7. C. H. Yeh, C. W. Chow, C. H. Wang, F. Y. Shih, Y. F. Wu, and S. Chi, "Using four wavelength-multiplexed self-seeding Fabry-Perot lasers for 10 Gbps upstream traffic in TDM-PON," *Opt. Express* **16**(23), 18857–18862 (2008).
8. C. H. Yeh, F. Y. Shih, C. H. Wang, C. W. Chow, and S. Chi, "Cost-effective wavelength-tunable fiber laser using self-seeding Fabry-Perot laser diode," *Opt. Express* **16**(1), 435–439 (2008).
9. D. J. Shin, D. K. Jung, H. S. Shin, J. W. Kwon, S. Hwang, Y. Oh, and C. Shim, "Hybrid WDM/TDM-PON with wavelength-selection-free transmitters," *J. Lightwave Technol.* **23**(1), 187–195 (2005).
10. G. Talli and P. D. Townsend, "Hybrid DWDM-TDM long-reach PON for next-generation optical access," *J. Lightwave Technol.* **24**(7), 2827–2834 (2006).
11. G. Kramer, B. Mukherjee, and G. Pesavento, "Interleaved polling with adaptive cycle time (IPACT): a dynamic bandwidth distribution scheme in an optical access network," *Photonic Netw. Commun.* **4**(1), 89–107 (2002).
12. T. Amano, F. Koyama, T. Hino, M. Arai, and A. Mastutani, "Design and fabrication of GaAs-GaAlAs micromachined tunable filter with thermal strain control," *J. Lightwave Technol.* **21**(3), 596–601 (2003).
13. M. Schell, D. Huhse, W. Utz, J. Kaessner, D. Bimberg, and I. S. Tarasov, "Jitter and dynamics of self-seeded Fabry-Perot laser diodes," *IEEE J. Sel. Top. Quantum Electron.* **1**(2), 528–534 (1995).
14. M. P. McGarry, M. Reisslein, and M. Maier, "WDM Ethernet passive optical networks," *IEEE Commun. Mag.* **44**(2), 15–22 (2006).

1. Introduction

Time division multiplexed passive optical network (TDM-PON) such as Ethernet PON (EPON) and Gigabit PON (GPON) is a promising solution in the last mile access systems and have being deployed around the world [1,2]. However, the introduction of bandwidth-intensive applications such as IPTV, HDTV and video-on-demand (VOD) will push the per-user capacity in such PONs to its limits as a single wavelength channel is shared among all users. Hence, 10 Gbps TDM-PONs are investigated in order to satisfy higher capacity requirements [3]. The 10 Gbps downstream transmitter can be deployed easily using distributed feedback laser diode (DFB-LD) with external modulation. But 10 Gbps upstream burst mode transceivers is expensive and not practical in the near future, since the cost of the optical network unit (ONU) is paid solely by each user.

In order to avoid higher upstream burst mode transceivers, increasing the number of upstream wavelength channels in TDM-PON for upstream capacity upgrade is a promising approach [4–7]. Some schemes have been reported either using tunable lasers or multiple continuous wave (CW) laser sources with tunable filters at the ONU [4,5]. These schemes, however, can be costly and complex to implement and also would require external modulators. M. Attygalle et al. presented a single Fabry-Perot Laser Diode (FP-LD) as the channel selector and burst mode transmitter for upstream transmission by strategically tuning the temperature of FP-LD [6]. But the realization of the accurate temperature tuning is very difficult and hence is very expensive. Chien-Hung Yeh et al. also proposed to simultaneously utilize four wavelength-multiplexed self-seeding directly modulated FP-LDs in each ONU acting as the upstream signal transmitter to increase upstream bandwidth [7]. However, the simple scheme is lack of flexibility in scheduling wavelengths and has lower resource utilization especially for those light-load ONUs.

In this paper, we presented a novel Upstream Multi-Wavelength Shared (UMWS) PON architecture, based on some novel configurations of wavelength-tunable self-seeding Fabry-Perot Laser Diode (FP-LD) without fiber amplifiers inside the gain cavity at ONUs. The single-longitudinal-mode (SLM) output of the proposed tunable laser module at ONUs is implemented via the optical injection and feedback scheme of the FP-LD. Hence, it does not require external light injection sending from the optical line terminal (OLT) and dynamically locks onto one of many longitudinal modes of the FP-LD by using a simple Sagnac fiber loop or a circulator-based fiber loop as a light reflector, instead of fiber reflective mirror (FRM) [8].

The proposed UMWS PON is believed to be a promising candidate for the next generation access network thanks to the following reasons. First, the PON provides an advantage of simply upgrading the present TDM-PON in the upstream capacity by introducing multiple wavelengths (to avoid higher burst mode data speed at ONUs) and keeping the fiber transmission link intact. Moreover, all ONUs share the all upstream wavelengths to transfer upstream data with a wavelength or finer sub-wavelength granularity, which improves significantly bandwidth utilization with inter-channel statistical multiplexing (via wavelength channel switch). Last but not least, the UMWS PON also presents a cautious upgrade path in that wavelength channels can be added on the user demand. More precisely, only ONUs with higher traffic demands may be upgraded by deploying proposed self-seeding laser module, while ONUs with lower traffic demands remain unaffected. Thus, a single-channel TDM-PON can be upgraded alternatively into a heterogeneous WDM (wavelength division multiplexed) /TDM PON in which the ONUs differ in upstream capabilities.

The rest of the paper is organized as follows. Section 2 shows the proposed UMWS PON architecture and describes the operation principle of the ONU tunable laser module based on the self-seeding FP-LD. Section 3 demonstrates the output performances of the laser module such as wavelength and power stability, side-mode suppression ratio (SMSR), tuning range, and bit-error-rate (BER) with direct modulation of 1.25 Gbps upstream data. A power budget

analysis for the upstream data was carried out to verify the feasibility of the upstream link. In section 4, we not only evaluate the performance gained from the upstream wavelength-sharing compared with prevailing hybrid WDM/TDM PON [9,10], but also for the first time investigate the effect of channel switch latency (SL) on the PON performances with the multi-wavelength Interleaved Polling with Adaptive Cycle Time (WDM-IPACT) scheme [11]. The conclusions are given in Section 5.

2. Architecture design and operation principle

The UMWS PON architecture based on a tunable self-seeding FP-LD at ONU is shown in Fig. 1, where three ONU transmitter structures are displayed. In the OLT, a DFB-LD and a Mach-Zehnder modulator (MZM) are used to generate downstream broadcasting signal (λ_d) to each ONU. A $1 \times m$ wavelength de-multiplexer/multiplexer (WDM) and a bank of Photo-Detectors (PDs) are used to simultaneously receive signals in multiple upstream wavelengths. An optical amplifier EDFA (Erbium-doped fiber amplifier) is installed before WDM to compensate the upstream transmission loss and to improve the power budget. In Remote Node (RN), a $1 \times n$ optical splitter is applied to split downstream carrier (λ_d) power to each ONU and to combine multiple upstream wavelengths (λ_{1u} to λ_{mu}) sent back to OLT, respectively.

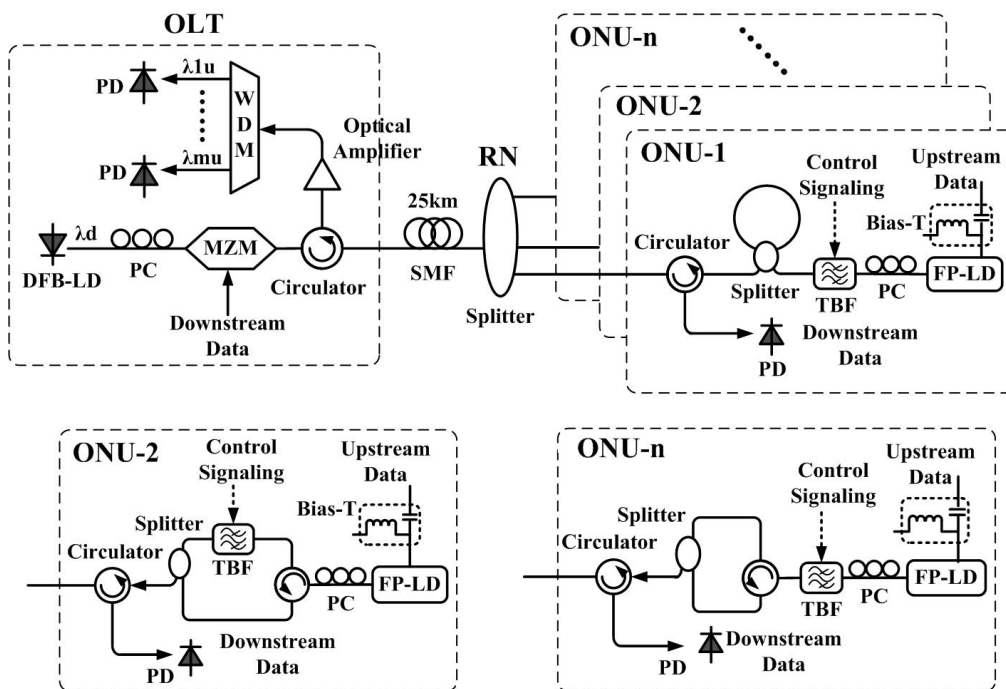


Fig. 1. Proposed UMWS-PON system based on a tunable self-seeding FP-LD at ONUs. Three ONU transmitter structures are displayed in the inset ONU-1, ONU-2, ONU-n, respectively.

In ONU, we use an optical circulator to connect an upstream transmitter and a PD as a downstream receiver. Here, we proposed three different structures of upstream transmitter at ONU. The three structures have same function components: 1) a FP-LD as an original light source with multi-longitudinal-mode (MLM) output, 2) a tunable band-pass filter (TBF) used to dynamically filter a designated single longitudinal mode (SLM), and 3) a feedback device for self-seeding FP-LD to produce a power-constant SLM output. The main difference of the three transmitter structures lies in the realization of the feedback device. In the inset ONU-1, we utilize a 2×2 optical coupler to construct a Sagnac fiber loop reflector as a feedback device for self-seeding FP-LD. In the inset ONU-2 and ONU-n, an optical circulator is linked to a 1×2 optical coupler to form a fiber loop reflector, and another port of the 1×2 optical

coupler serves as an output of the fiber laser module. The TBF can be positioned either inside the fiber loop (e.g. in ONU-2), or before the fiber loop (e.g. in ONU-n).

The FP-LD has MLM output with ~45% front-facet reflectivity. The TBF is required to be capable of precisely changing their center wavelength according to a voltage signal. For example, micro-machined vertical cavity filters using multiple distributed Bragg reflectors (DBR) can be used for these tunable filters, which have fast tuning responses and wide wavelength tuning range with low tuning voltages [12]. Once the ONU receives the downstream control signal from the OLT on the assigned wavelength channel, the control circuits on the ONU are triggered for the TBF calibration. Thus, the MLM FP-LD is aligned to the certain filter mode of the TBF. The filtered longitudinal mode will be reflected by the feedback device and injected back into the FP-LD. Therefore, the feedback light is selected by the TBF and transmits through the following fiber path: FP-LD → TBF → feedback device → TBF → FP-LD → TBF → feedback device → Output. Hence, the FP-LD will laser at single longitudinal mode and the optical SLM output is amplified by self-seeding operation.

Based on the self-seeding operation scheme, upstream signal can be obtained by directly modulating the FP-LD in arbitrary wavelength by dynamically adjusting the TBF. The polarization controller (PC) is placed inside the gain cavity to control the polarization state of the feedback light into the FP-LD properly, obtain maximum output power, and maintain wavelength stabilization. The injected light at the state of the TE mode of FP-LD will result in the maximum injection locking efficiency [13]. Some control schemes such as temperature and wavelength control are also required so to ensure nearly the same set of wavelengths can be produced by different ONUs. Furthermore, a dynamic bandwidth allocation (DBA) scheduler with two-dimension schedule functions for time and wavelength resources can be equipped at the OLT to allow efficient sharing of upstream wavelength resource with all ONUs. We note that network operators are expected to deploy only a small number ($m = 3$ or 4) of extended wavelengths and incremental upgrades [14]. Hence, the number m of extended wavelengths is usually smaller than the number n of ONUs. The transmission in the PON infrastructure is totally 25km single mode fiber (SMF) without dispersion compensation.

3. Experiment and results

In the section, we experimentally investigate the proposed self-seeding laser module at ONU. Because the three different structures of ONU upstream transmitter have same operation principle and similar experiment results, we just illustrate the experimental results of the ONU-1 structure in Fig. 1 for the paper conciseness. In the proof-of-principle experiment, we use 1.5 μ m FP-LD with 1.25G modulation bandwidth to simulate the unavailable 1.3 μ m FP-LD in our lab.

Figure 2(a) shows the free-running output spectrum of the MLM FP-LD without self-seeding when the bias current and temperature are 30mA and 250C respectively. The TBF has a 3-dB bandwidth of 0.4nm and a ~3.5dB insertion loss. Thus, the MLM FP-LD is aligned to the certain filter mode of the TBF. The filtered single longitudinal mode will be reflected by the Sagnac fiber loop and injected back into the FP-LD. It is worth noting that the Sagnac fiber loop is composed of an optical coupler with the maximum splitter ratio (90:10), which provides 90% power for the output and 10% for the feedback to the FP-LD, to enhance output power of the proposed self-seeding FP-LD module. It is due to fact that a 50:50, 30:70 or 20:80 optical coupler will lead to the lower output power via experimental investigations. While the TBF is set at 1553.86nm, the stable SLM output is shown in Fig. 2(b). Figure 2(c) presents the complex output power spectra of the proposed laser module in the tuning range of 1544.69nm to 1563.39nm with the tuning step of ~1.34nm.

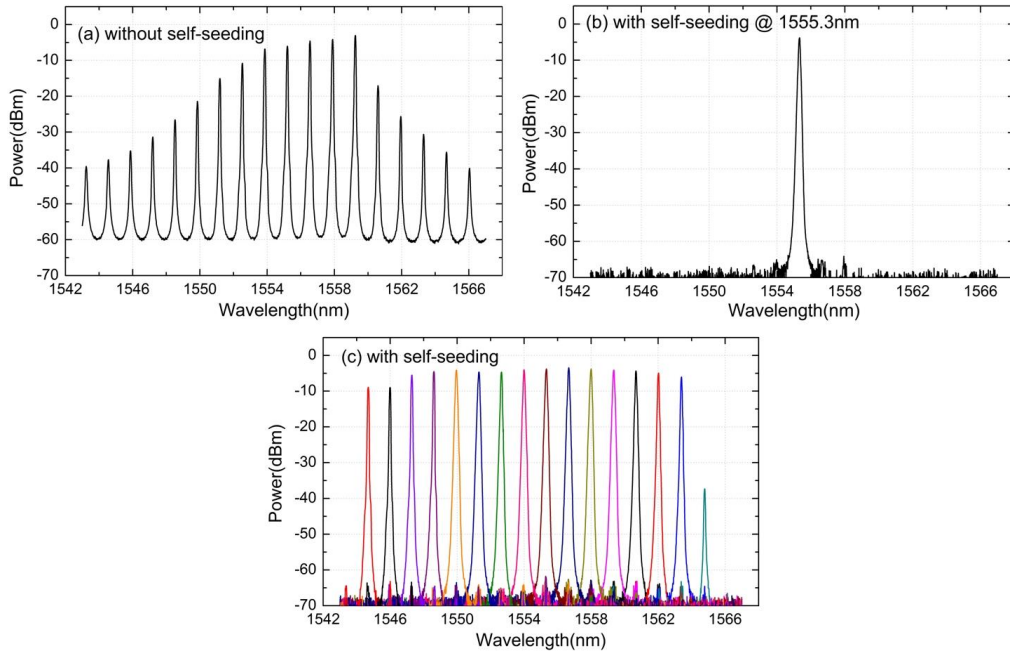


Fig. 2. (a) Original output spectrum of MLM FP-LD operated at 30 mA in the temperature of 25°C. (b) SLM output is obtained while the TBF is set at 1555.3nm. (c) Complex output spectra of proposed laser module in the wavelength range of 1544.69nm–1563.39 nm with tuning step of 1.34 nm.

Figure 3(a) shows the output power and SMSR versus the different lasing wavelengths with ~1.34-nm tuning step. The maximum output power of -3.4 dBm is at the wavelength of 1546.0 nm. The minimum output power is -9.0 dBm at 1556.69 nm. The maximal output power difference ΔP_{\max} is about 5.6 dB. When the lasing wavelength is 1556.69 nm, the SMSR can reach 71.4 dB. The minimum of SMSR is 65.5 dB at 1544.96-nmwavelength ($\Delta \text{SMSR}_{\max} = 5.9$ dB). The output power of the laser is determined by the gain profile of the FP-LD, hence it is lower at both ends of the spectrum.

To investigate the output performances of power and wavelength stabilities, a short-term stability of ONU-1 is measured. Initially, the lasing wavelength is 1554.08 nm and the observing time is over 30 min. In Fig. 3(b), the wavelength variation and the power fluctuation are 0.05 nm and 1.37 dB, respectively. After two-hour observing, the stabilized output is still maintained. As a result, the proposed wavelength-tunable fiber laser at ONUs has the advantage of simple configuration, high output efficiency, and wide wavelength tuning range.

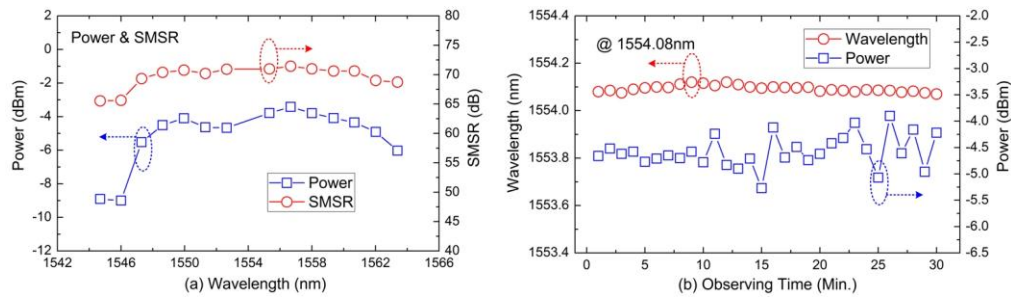


Fig. 3. (a) Output power and SMSR spectra in the wavelength range of 1544.69nm–1563.39 nm with a 1.34nm tuning step. (b) Output variations of central wavelength and power at 1554.08 nm over 30 min.

Figure 4 presents the BER measurements and eye diagram of the 1.25Gbps upstream signals at the lasing wavelength of 1554.08nm in the case of back-to-back (BTB) and after 25-km transmission without dispersion compensation. The power penalty is less than 0.2 dB.

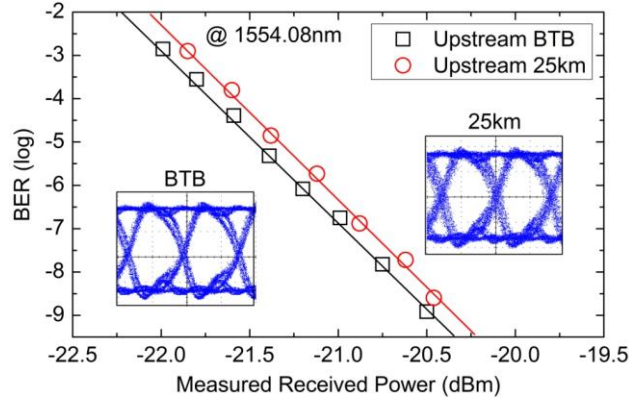


Fig. 4. BER and eye diagrams for the upstream traffic with BTB and 25km transmission.

To verify the feasibility of the upstream link using the proposed tunable self-seeding laser with different split ratios in the network, a power budget analysis for the upstream data was carried out using the minimum output power of around -9 dBm at ONU (Fig. 3(a)). The EDFA gain reached about 30 dB in OLT to compensate the upstream transmission loss and to improve the power budget. The receiver sensitivity of the upstream data was considered to be -20.4 dBm according to the experimental data (Fig. 4). In this analysis, the total loss except for the optical coupler at RN consist of a 0.8-dB insert loss for the optical circulator at ONU, a 0.2 dB/km transmission loss for a 25-km optical fiber, a 5-dB insert loss for WDM and a 0.8-dB optical circulator loss at OLT. When the split ratio is 8, 16, 32, 64, the optical coupler loss at RN is 11, 14, 17, 21-dB, respectively, where the insertion loss of the coupler is 2-dB and a 3-dB loss for each 1×2 power-split. The power margins shown in Table 1 indicate the feasibility of the larger split ratio and transmission scope in the proposed UMWS PON.

Table 1. Power Margin Calculation for Upstream Data with Different Split Ratios

| Split Ratio | 8 | 16 | 32 | 64 | 128 |
|-----------------------------------|-------|-------|-------|-------|-------|
| Minimum output power at ONU (dBm) | -9 | -9 | -9 | -9 | -9 |
| EDFA amplifier gain (dB) | 30 | 30 | 30 | 30 | 30 |
| Receiver sensitivity (dBm) | -20.4 | -20.4 | -20.4 | -20.4 | -20.4 |
| Other insertion losses (dB) | 11.6 | 11.6 | 11.6 | 11.6 | 11.6 |
| Optical coupler loss at RN (dB) | 11 | 14 | 17 | 21 | 24 |
| Power Margin (dB) | 18.8 | 15.8 | 12.8 | 9.8 | 6.8 |

4. Performance analysis and simulation results

In the proposed UMWS PON, we assume that all ONUs can have full access to all upstream wavelengths, and are equipped with the proposed tunable self-seeding FP-LD module. Thus each ONU can switch any designed wavelength channel according to the OLT scheduling information. We note that the channel switch is realized via a tunable filter, which has tuning times in the scale of microseconds [12]. Hence, the filter tuning time cannot be neglected compared with the transmission time of a data packet with the packet length ranging from 64 to 1518 bytes on a 1Gbps link. Therefore, in the following simulations we not only evaluate the performance merit gained from the flexible sharing of the multiple upstream wavelength resources, but also for the first time investigate the impact of channel Switch Latency (SL) on the network performance.

In the upstream bandwidth allocation, decisions both on when and for how long (*Timeslot*) and on which *Wavelength* channel to grant an ONU upstream transmission are required to make efficient use of the upstream bandwidth. To solve the joint *Wavelength* and *Timeslot* Scheduling (WATS) problem, we consider an online scheduling strategy in the paper based on the multi-wavelength Interleaved Polling with Adaptive Cycle Time (IPACT) [11] scheme. The OLT online scheduler schedules ONUs one-by-one without considering the bandwidth requirements of other ONUs. It schedules an ONU to transmit on the first available wavelength channel (FAWC) supported by that ONU, within a designed timeslot with window size purely according to the reported size in the previous Request message, as long as it has not exceeded the maximum window limit. In other words, we adopt the FAWC scheme in choosing wavelength channel, and the Limited assignment scheme [11] is used to prevent the upstream channel monopolization by one ONU with high data volume.

In this simulation, an UMWS PON is consisting of an OLT and N ONUs with m upstream wavelength channels. The Round Trip Time (RTT) delay for each ONU is assumed to be randomly (uniformly) over the interval $[25\mu\text{s}, 100\mu\text{s}]$, which corresponds to the distance between OLT and ONUs ranging from 5 to 20 km. The access link data rate from users to an ONU is 100Mbps. The upstream rate of each wavelength channel is 1Gbps. The ONU buffer size is 10Mbytes. The upper bound limitation of transmission window length is 15000 Bytes when the Limited assignment scheme is adopt. The ONU traffic load follows the self-similar traffic source model [15], which is simulated by alternating Pareto-distributed ON/OFF source model. The shape parameter α is 1.4 and the Hurst parameter can be calculated by $H = (3-\alpha)/2 = 0.8$. The above simulation parameters are concluded in Table 2. For each simulation case, each scheduling result is the average over 100 simulations.

Table 2. Reference System Simulation Parameters

| Parameters | Reference Value |
|---|----------------------|
| ONU number n^* | 64 or 32 or [16, 64] |
| Number m of upstream wavelength in a PON* | 4 or 3 |
| Link data rate from users to an ONU | 100Mbps |
| Upstream rate of each wavelength channel | 1Gbps |
| ONU buffer size | 10Mbytes |
| Distance between the OLT and ONUs | [5, 20] -km |
| Upper bound limitation of transmission window | 15000 Bytes |

*Different values are taken in different simulation scenarios.

4.1. Performance gain of the upstream wavelength sharing

In the first simulation, we just evaluate the enhanced performance of the proposed UMWS PON compared with the prevailing TDM-over-WDM PON [9,10] without taking the channel Switch Latency (SL) into consideration. In UMWS PON, 64 ONUs share 4 upstream wavelengths by using the tunable self-seeding FP-LD module at each ONU. In the conventional TDM-over-WDM PON, all ONUs are grouped to 4 TDM-sub-PONs each containing 16 ONUs and a fixed upstream wavelength. Let $load_i^{ave}$ be the average traffic load from ONU- i ; $load_i^{max}$ be the maximum admitted traffic load of ONU- i . We define the traffic Load Heterogeneity of ONU- i as follows:

$$Load_Heterogeneity_i = load_i^{max} / load_i^{ave} \quad (1)$$

We consider five types of traffic load profile for each ONU: each type has the identical average traffic load ($load_i^{ave} = 0.5$) and different load heterogeneities ($Load_Heterogeneity_i = 1, 1.2, 1.4, 1.6, \text{ and } 1.8$), respectively.

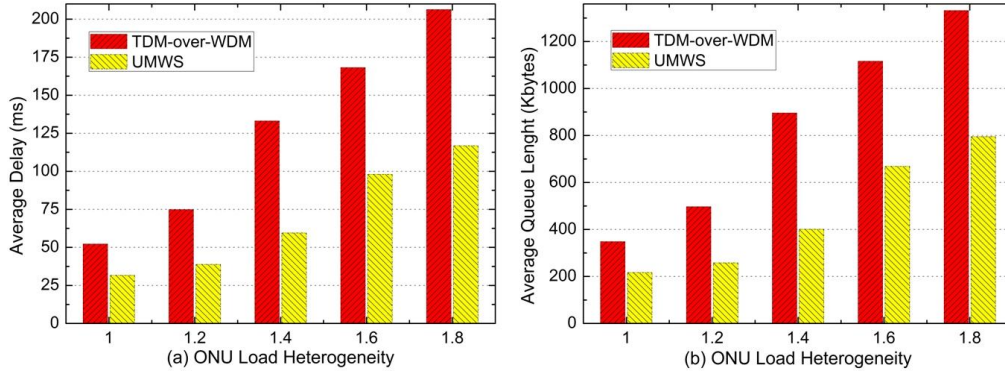


Fig. 5. Performance gain of UMWS PON in the (a) Average Delay and (b) Average Queue length compared with the conventional TDM-over-WDM PON.

Figure 5 shows that the proposed UMWS PON significantly outperforms the conventional TDM-over-WDM PON in the Average Delay and Average Queue length, which is primarily due to the sharing and flexible scheduling of upstream wavelength resource among all ONUs. We also note that as the heterogeneity of ONU traffic load becomes larger, the performance gain is increasing obvious. This signifies the UMWS PON can provide better performances in a more practical network scenario having heterogeneous traffic load.

4.2. Performance impact of Switch Latency under different ONU traffic loads

In the simulation, the impact of the channel Switch Latency (SL) on the network performance is investigated under different ONU traffic load ranging from 0.1 to 0.9. We assume that all 32 ONUs have identical traffic load and 3 upstream wavelengths are available in a PON. We define the Channel Switch Ratio (CSR) as the number of channel switch times divided by the total number of GATE messages sent in a simulation lasting 20s running time, as shown in Eq. (2). We first illustrate the CSR performances to facilitate to explain thoroughly other network performance parameters such as average delay and packet loss ratio.

$$CSR = \frac{\text{Number of channel switch times}}{\text{Number of GATE messages}} \quad (\text{during 20s simulation time}) \quad (2)$$

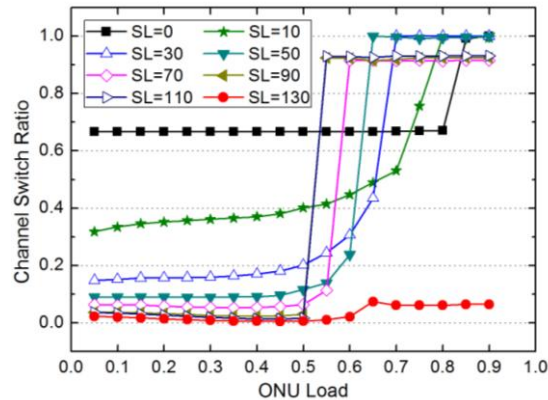


Fig. 6. Channel Switch Ratio (CSR) with different SL values under the ONU load variations.

Figure 6 depicts the CSR versus ONU load with different SL values. We take the $SL = 0$ case as performance baseline, which corresponds to an ideal wavelength-sharing PON without channel SL consideration. For the $SL = 130$ case, the CSR is always very low. The SL value is so large that it is equivalent to the largest transmission window length on a 1Gbps upstream

link (that is $15000\text{Bytes} * 8 / 1\text{Gbps} = 120\mu\text{s}$). This situation reduces significantly the channel switch time nearly to zero, which is similar to a static wavelength-allocation PON without any channel switch action.

For other SL cases, we observe that the CSR remains almost constant at the light loads and abruptly reaches the highest value at the heavy loads. The reason is that the lower load makes the earliest available time of different wavelength channels closer to each other and hence the channel switch is not necessary. At the heavier load, the earliest available times of each wavelength channel become quite different, which makes the channel switch turn to be more frequent. We also find that as the SL value increases, the CSR become smaller at light load but reaches the highest value earlier at heavy loads. It is due to the fact that the higher SL tends to reduce channel switch times at lighter load, but as the ONU load increases, the higher SL introduces more delay, which leads to more frequently switch the upstream channel.

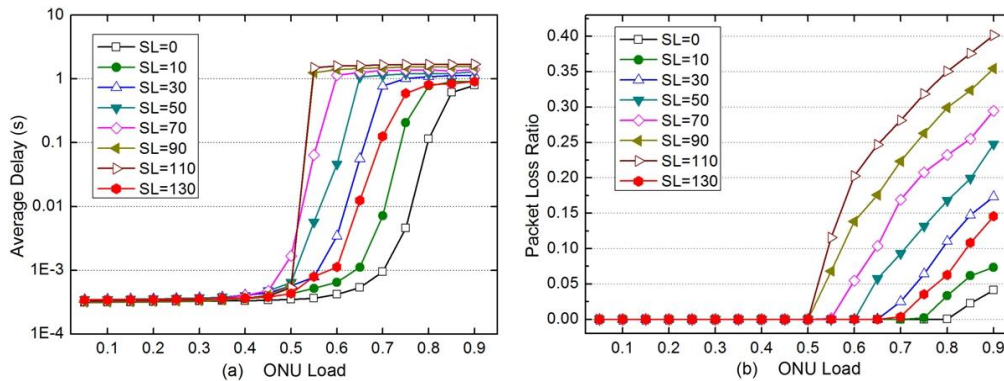


Fig. 7. (a) Average delay and (b) packet loss ratio versus the ONU load with different SL values.

Figures 7(a) and 7(b) show the average packet delay and packet loss ratio with the ONU load variation respectively. We observe that at the light load less than 0.5, the average packet delay preserves a very low value for all SL cases, which leads to the nearly zero packet loss ratio. But when the ONU load is larger than 0.5, different SL curves separate each other. The higher the SL is, the larger average delay becomes and the earlier average delay reaches the maximal value. It results from the fact that CSR also reaches the highest value earlier as shown in Fig. 7. Because the larger packet delay will give rise to higher packet loss ratio, Fig. 7(b) displays the same trend as Fig. 7(a). It is noted that the SL = 130 performance is better than SL = 30 case. This result indicates the larger SL seriously spoils the upstream performances. Just when the SL is small enough (less than $30\mu\text{s}$), the performance gain mentioned above can appear compared with a static wavelength-allocation PON, which is corresponding to the SL = 130 case.

4.3. Performance impact of Switch Latency under varied on-line ONU numbers

In the simulation, we vary the on-line ONU numbers from 16 to 64, and randomly set each ONU load chosen from the interval [0.1, 0.9]. There are 3 upstream wavelength channels to be used in a PON. In the same way, we first illustrate the CSR performances to study the impact of the channel SL on the network performance.

Figure 8 shows the CSR of different SL values under the random traffic load and varied on-line ONU number. We find that the CSR decreases as SL increase. When SL = 0, the CSR has almost no difference at about 0.67 and while the SL = 130 the CSR is very small below 0.1. It is because the larger SL tends to prevent channel switch at certain degree. We also observe that the increase in the on-line ONU number represents the heavier network traffic load, which consequently leads to a slow rise of the CSR curve.

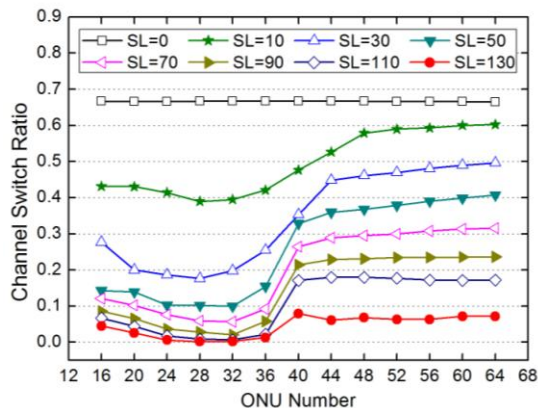


Fig. 8. Channel Switch Ratio (CSR) versus on-line ONU number with different ONU load.

From Fig. 9, we observe that when the on-line ONU number is smaller, the average packet delay is also a very low value, and the packet loss ratio is nearly zero for all SL cases. But for the larger on-line ONU number, different SL curves separate each other. The higher the SL is, the larger average delay and the higher packet loss ratio become. We also note that the performance for SL = 130 case is slightly better than that for the SL values of more than 50 μ s. We know that the SL = 130 curve represents the performance of a static wavelength-allocation PON. So we have same conclusion as in Fig. 7 that the performance gained from dynamic wavelength allocation scheme is obtain only when the SL is small enough (about 30 μ s), which is the 25% of the maximal admitted transmission window.

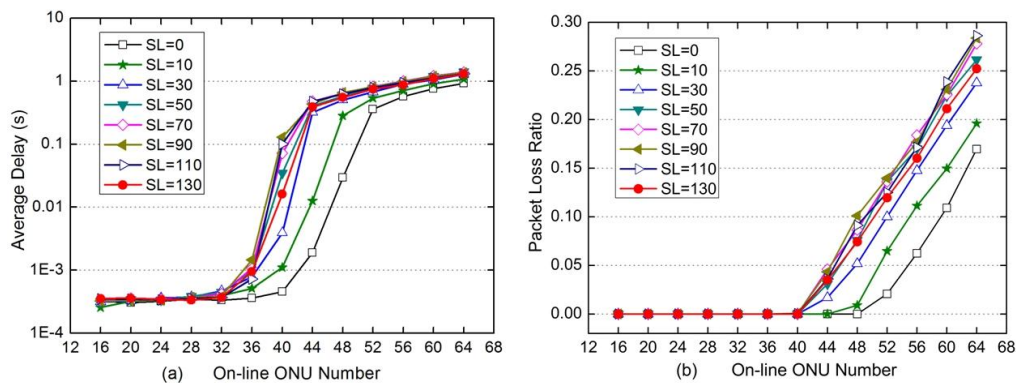


Fig. 9. (a) Average delay and (b) Packet loss ratio versus the on-line ONU number under different ONU load.

5. Conclusion

We propose a novel UMWS PON architecture based on the tunable self-seeding FP-LD module at ONU. The PON not only upgrades easily upstream capacity by introducing multiple wavelengths (to avoid higher burst mode data speed at ONUs), but also improves significantly bandwidth utilization with inter-channel statistical multiplexing. The outputs of the self-seeding FP-LD module have a good performance of output power, optical SMSR and stabilities in the wavelength tuning range of 1547.18nm to 1561.92nm with tuning step of 1.34 nm via experimental investigation. The BER measurement is performed for 1.25Gbps upstream data. With the proposed PON infrastructure, we not only evaluate the performance gained from the flexible sharing of the multiple upstream wavelength resources, but also for the first time investigate the impact of channel SL on the network performance. The extensive simulations show that the enhanced performance is obtained just under the condition that the

channel SL is small enough. Therefore we believe that the UMWS PON would be a promising solution for next generation access networks as the development of advanced optical commutation technologies.

Acknowledgment

The work was jointly supported by the National Natural Science Foundation of China (NSFC) (No. 60972032 and No. 61071080) and China 973 program under grants 2010CB328204 and 2010CB328205.